A Personal Identification System Using Iris Recognition

Naba Jassim Muhammad
Sorour Naseer Mohammed
Hadeer Muhannad Adnan

Department of Computer Science
University Diyala University
City, Iraq

ABSTRACT

One of the promising biometric recognition method is Iris recognition. This is because the iris texture provides many features such as freckles, coronas, stripes, furrows, crypts, etc. Those features are unique for different people and distinguishable. Such unique features in the anatomical structure of the iris make it possible the differentiation among individuals. So during last year's huge number of people have been trying to improve its performance. In this article first different common steps for the Iris recognition system is explained. Then a special type of neural network is used for recognition part. Experimental results show high accuracy can be obtained especially when the primary steps are done well.

KEYWORDS

iris recognition, biometric identification, pattern recognition, automatic segmentation.

الاهداء

الى ذلك الحب الذي لا يتوقف و ذلك العطاء الذي لا ينضب الى وطني الحبيب الى بؤرة النور التي عبرت بي نحو الأمل و الأماني الجميلة و اتسع قلبه ليحتوي حلمي حين ضاقت الدنيا و علمني معنى أن نعيش من أجل الحق و العلم حتى لو كان على حساب ارواحنا واهديه الى امي العزيزة الى رفيقة دربي الطويل معيني بعد الله عز و جل في هذه الحياة يطولي الله في عمرها ويحفظها لي

شكر و تقدير

الشكر الأول هو الله عز وجل ثم والدي
ووالدتي على كل مجهوداتهم منذ
ولادتي إلى هذه اللحظات ، أنتم كل
شيء بالنسبة لي أحبكم يسرني أن
أوجه شكري لكل من نصحني أو
أرشدني أو وجهني أو ساهم معي
في إعداد هذا البحث بإيصالي
للمراجع والمصادر المطلوبة في أي
مرحلة من مراحله . شكر خاص
لمشرف البحث [د . جمال مصطفى]
شكر خاص لكل اساتذة كلية العلوم -
قسم علوم الحاسبات المحترمين.

1. INTRODUCTION

1.1 Biometric in general

Biometrics refers to the identification of human identity via special physiological traits. So scientists have been trying to find solution for designing technologies that can analysis those traits and ultimately distinguish between different people. Some of popular Biometric characteristic are features in fingerprint, speech, DNA, face and different part of it and hand gesture. Among those method face recognition and speaker recognition have been considered more than other during last 2 decades. The idea of automated iris recognition has been proposed firstly by Flom and Safir. They showed that Iris is an accurate and reliable code in biometric identification.First of all iris isan internal part of the body that can be seen easily. Also visible patterns are unique for each individual person. So it is really hard to find two person with identical iris pattern. Also iris pattern even for left and right eyes are different.Moreover those pattern are almost fix and not going to change during life. So the patterns of the iris are almost constant during a person's lifetime.As a result by use of a features that are highly unique the chance of having two individual having the same features is minimal. Considering those uniqueness and proposing algorithm to could extract iris correctly would lead to stable and accurate system for solving human identification problem. Although some new researches revealed there are some methods to hack this type of systems(such as capturing image form person Iris in press conference), still iris recognition is a reliable human identification technique and reliable security recognition system. For this research we not going to capture new image by camera, instead a famous data set (CASIA database [1]) is used to evaluate results. This dataset contains thousands of different images and publicly is available upon request.

1.2 Background

Alphonse Bertillon and Frank Burch who were ophthalmologistproposed that iris patterns can be a reliable method for identification systems [2, 13] while John Daugman [3] was the first person that invent a system for the identification verification based on irispatterrn. Another valuable work proposed by R.Wildes et al. Their method was different both in the algorithm for extracting iris code and the pattern matching technique. Since the Daugman system has been shown high performance and really low failure rate, his systems are patented by the Iriscan Inc. and are also being commercially used in Iridian technologies, British Telecom, UK National Physical Lab etc. So in our research, the Daugman model is used for extracting iris pattern. Besides using common steps used in other works such as image acquisition and pre-processing, iris localization and normalization, our research utilize a powerful neural networks, say LAMSTAR [9] for recognition part. Because of availability of Daugman model [6, 7] and related source code a quick review is provided in each section todescribe the theoretical approach and their results. The paper mainly focused on used neural network and its implementation along withinitial experimental result and suggestion for improve of performance.

1.3 Image acquisition

To have a reasonable result, this step should be done accurately. Having a high quality image with minimal level of noise reduce the necessary procedure for noise reduction and promote other step's result.. Especially when image are taken closely error originated from different steps would be reduced due to removing reflection effect. To focus on our method that is actually a special type of classifier, uses the image provided by CASIA (Institute of Automation, Chinese Academy of Sciences) are used as a data set. These images were taken for the purpose of iris recognition software research and implementation. Due to using Infra-red light for illuminating the eye specular reflections effect has been reduced in this data set.So here some initial steps for decreasing error originated from reflection is not necessary. It is clear that for real-time application reflection removal process is needed.

2. IRIS LOCALIZATION

2.1 Method

The part of the eye containing information is only the iris region. As is shown iris is located between the sclera and the pupil. So it is necessary to get the iris from eye image. Actually a segmentation algorithm should be used to find the inner and outer boundaries. There are huge number of research for image segmentation such as [5]or that is based on more sophisticated algorithm but the most popular method for segmentation is edge detection. For this purpose Cany edge detector has been shown successful. The Canny detector mainly have three main steps that are finding the gradient, non-maximum suppression and the hysteresis thresholding [8,11]. As proposed by Wildes, by considering the thresholdin a vertical direction the effect of the eyelids would be decreased. Knowing that applying this method remove some pixels on the circle boundary, an extra step that is actually Hough transform would lead to successful localization of the boundary even with absence of those pixels. Also computational cost is lowerbecause the boundary pixels are lesser for calculation. The procedure is summarized to following steps. For a pixel gradian_image(x,y), in the gradient image, and given the orientation theta(x,y), the edge intersects two of its 8 connected neighbours. The point in (x,y) is a maximum if its not smaller than the values of the two intersection points.By applying next step sayinghysteresis thresholding, the weak edges below a low threshold would be eliminated, but not if they are connected to an edge above a high threshold through a chain of pixels all above the low threshold. On the other hand the pixels above a threshold T1should be separated. Then, these points are marked as edge points only if all its surrounding pixels are greater than another threshold T2. The values for threshold were foundtentatively by trial and error, and are 0.2 and 0.19 according to

2.2 Normalization

Extracted iris has different size and value. To feed this pattern to a classifier all pattern should be normalized. To normalizationan iris regions a method that is called Daugman's rubber sheet model [6,7] has been used. In this methodcentre of the pupil is used as the reference point and radial vectors pass through the iris region. The procedure is shown in Figure 1. A number of data points are selected along each radial line and this is called the radial resolution. Also the number of radial lines going around the iris is calledthe angular resolution. Since sometimes the pupil can be non-concentric respect to the iris, a procedure that is called remapping must be utilizedto rescale points based on the angle

around the circle.
This is given by

$$r' = \sqrt{\alpha}\beta \pm \sqrt{\alpha\beta^2 - \alpha - r_I^2} \qquad (1)$$

with

$$\alpha = o_x^2 + o_y^2$$

$$\beta = \cos\left(\pi - \arctan\left(\frac{o_y}{o_x}\right) - \theta\right)$$

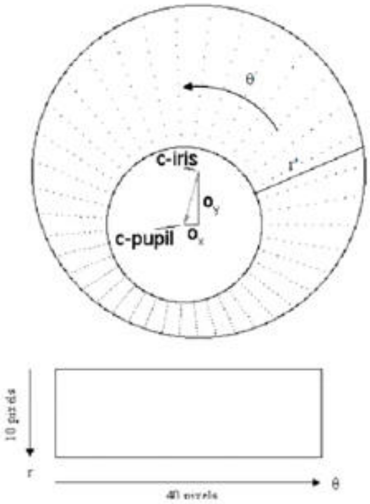

Figure 1

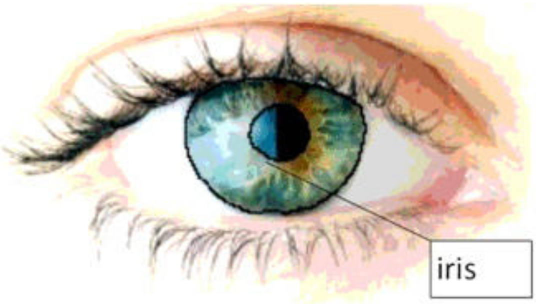

Figure 2. Result of iris localization

Here the displacement of the centre of the pupil relative to the centre of the iris is given byo_s
,$o_y$while r’ is the distance between the edge of the iris and edge of the pupil at an angle, θ around the region. Alsor_I is the radius of the irissuch asFig (1). The remapping equation first gives the radius of the iris region as a function of the angle θ. A constant number of points are chosen along each radial line, then a constant number of radial data points are taken at a particular angle. The normalized pattern was made by transferring the radial and angular position in the normalized patternto the Cartesian coordinates of data points. From the ‘Doughnut’ iris region, normalizationgenerate a 2D array with horizontal dimensions of angular resolution and vertical dimensions of radial resolution. The result for iris localization isshown in Fig (2). In this section all the procedure is the same as [10] model including removing rotational inconsistencies that is done at the matching stage based on Daugman’s rubber sheet model.

2.3 Results of localization and normalization

The result of normalizationstep based on mentioned methodshowed to be liable like some results shown in Figure 3.But, the normalization was not able to reconstruct the same pattern perfectly from images with changingof pupil dilation. This means that deformation of the iris results in small changes of its surface patterns. For example consider situation that the pupil is smaller in one image respect to another. Thenormalization process rescales the iris region to reach to constant dimension. Here, the rectangular representation is made by 10,000 data points in each iris. Until now the rotational inconsistencies have not been considered by the normalization. So the two normalized patterns are misaligned in theangular direction. The result of whole process is shown in fig (3). For all images in the folder the template is calculated that is actually a matrix. Size of matrix is 20×480. Then those matrix are saved to be used in future as a training set. This process is shown in figure (4).

Figure 3. resulting matrix after normalization

4. CLASSIF IER

In order to provide accurate recognition of individuals, neural network can be used. For this research a special neural networks has been used. So after makingour template and some initial steps mentioned before we have a matrix with the dimension of 20× 480. So for 16 number of class our classifier should be trained.In the next section implementation using LAMSTAR Neural network has been discussed. We decided to test it because it has been shown that is really powerful in other problems such as character recognition problem.

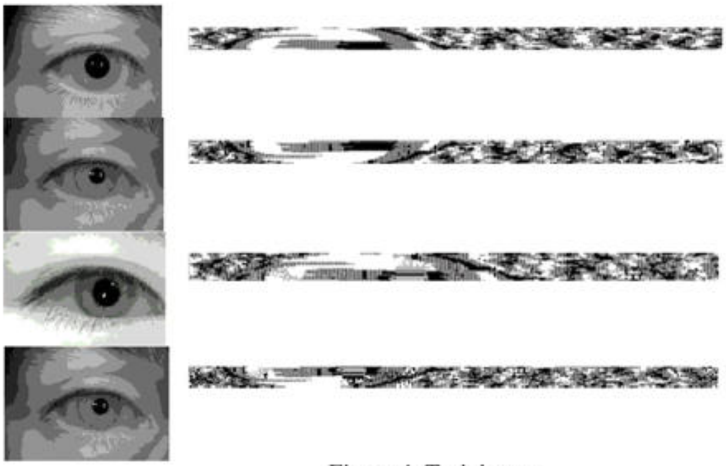

Figure 4. Training set

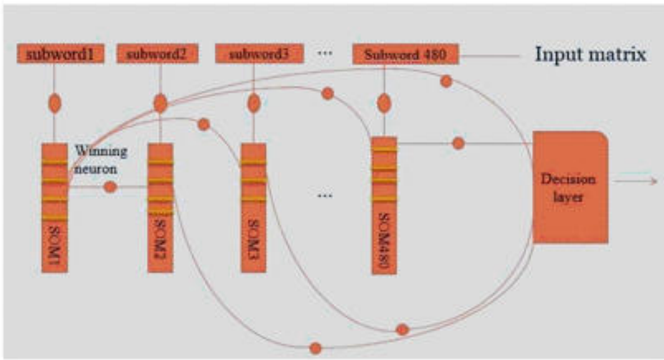

Figure 5. LAMSTAR structure

4.1 LAMSTAR neural network

4.1.1 Introduction to LAMSTAR

The problem consists in the realization of a LAMSTAR Artificial Neural Network for IRIS recognition. The LAMSTAR neural network, is a complex network, made by a modified version of Kohonen SOM modules. It doesn't need of the training. In fact, the input patterns are divided into many subwords, for example we considered columns of template as our subwords, so we have 480 subwords. These subwords are used for setting the weights of the SOM modules of the LAMSTAR. When a new input word is presented to the system, the LAMSTAR inspects all weights in

SOM. If any pattern matches to an input subword, it is declared as winning neuron for that particularly subword.The SOM-module is based on "Winner take All" neurons, so the winning neuron has an output of 1, while all other neurons in that SOM module have zero output.Here, the SOM is built statically.

This means that for every subword, we instantiate every time a new matrix that represents the SOM, and if computing the products between the stored weights and the input subword, we obtain a winner "1", we don't establish a new neuron. Otherwise, if computing that products, no one of the neurons that are present in the SOM module converge to "1", in other words, if we haven't a winner neuron, we instantiate a new neuron in the SOM module.

Every time that we instantiate a neuron, we normalize the new weights following the function such as [12, 15]:

$$x'_i = \frac{x_i}{\sqrt{\sum_j x_j^2}}$$

To converge the output of the winning neuron to "1" we follow the function below:

$$w(n+1) = w(n) + \alpha[X - w(n)]$$

Where $\alpha = 0.8$ and it is the learning constant, w is the weight at the input of the neuron, and x the subword.A particular case could happen: when the second training pattern is input to the system, this is given to the first neuron, and if its output is close to "1", another neuron isn't built. We create neurons only when a distinct subwordappears.The output layer is provided by the punishment and reward principle such as [14, 16]. If an output of the particular neuron is what is desired, the weight of the output layer is rewarded by an increment, while punishing it if the output is not what is desired.

We'll explain better this layer in the design section, reporting also the code for the sake of clarity.

4.1.2 Design

The design of the Neural Network is represented in the figure (5). In this network, we have 16 different representations for eyes which are both left and right eyes of 8 person. The input pattern is templates that has been extracted from images using last pre-processing steps. The size of those templates after normalization is 20×480.Here we considered each column as a word so each word is a vector with size of 20. Also for each person 5 different images is used for training.So we selected images from data set from folders that have more than 5 images for each case to could use reminder for the testing, So after making subwords, we normalize every subword with respect itself, as we said in the introduction section.After the normalization of the input subwords, we have to train the system starting from the SOM layer. We call a function every time that we change the subword. As we can read, we initialize the som_out (which is the current SOM module), and then if we haven't a winning neuron we create it (flag=0), Otherwise we take the current neuron as winning neuron.Once that the weights of the som modules are set (w_som), we proceed to the output training. This is complex because we have to look to the sum of all the weights between the winning neurons of the SOM modules and the output layer (they are firstly set to zero). If the sum of all the weightsis negative, we understand that result as "0". If is positive, we understand as "1". So the punishment and the reward is based on adding a small increment. Obviously for a negative sum, the punishment consist into adding a small positive increment, while the reward on adding a small negative increment. And vice versa for the positive sum. In this way, the system converges faster to the desired output if there's a reward, and it takes long if there's a punishment. Briefly, the algorithm follows this few steps:

1) Get the train patterns
2) Realize the subwords for every pattern
3) Normalize every subword
4) Set the weights of SOM module, creating every time a new neuron if it isn't a winning neuron for the new subword.
5) Set the output of the winning neuron to 1.
6) Set the weights of the Decision Layer to zero
7) Adjust the weights of last layer taking into account the desired output, with punishment and reward principle.

4.1.3) Normalized version of LAMSTAR

Based on the reward/punishment if in desire firing, a neuron is to be fired then the link weights will be rewarded. In case this happens for a couple of time the link weight value can be high enough to cause undesired neuron firing. To avoid this situation we use normalized LAMSTAR neural network in which we divide link weights by number of times the corresponding neuron was rewarded for desire firing. Considering advantages mentioned above we can add more positive points to LAMSTAR if we use the normalized version.Link weight of a neuron will not grow gradually if it wins much time.Convergence time will be reduced since normalization improve desired firing and Increase efficiency.

5. RESULT

The LAMSTAR and modified LAMSTAR are applied on CASIA interval database. Both of them are really fast. For instant required time for training was 66.1584s and for testing 2.5939 seconds while the accuracy was 99.39% for regular LAMSTAR and 99.57% for modified LAMSTAR. After tracing the program on each individual image I found pre-processing needs to be modified. Actually the performance of any classifier is directly depended to performance of algorithm used for finding template. For example rotational inconsistency should be taken into account. So steps including segmentation and normalization must be improved to be able to Get iris accurately and make template that is input of our neural network.It seems with having accurate templates the performance would be increased.

Algorithm	Recognition rate
Duagman	%98.58
LAMSTAR	%99.39
Modified LAMSTAR	%99.57

Table1. Comparison between performance of our proposed method and Duagman

6. CONCLUSION AND FUTURE WORK

In this work a new neural network method is presented for iris identification. A template is achieved using Image processing techniques. Classification is mainly done by LAMSTAR neural network. Structure of this network makes it a good candidate for classifying. The software code for image processing and the network has been written in MATLAB R2014a taking into account image processing toolbox and the fact that it is very user friendly in image processing application

After reprocessing step all template matrix are saved and in the next step they are loaded as input to classifier. Overall result suggests that normalized LAMSTAR increase efficiency and convergence time. The next step for increasing efficiency is considering rotational inconsistency. Also it seems that having a matrix with 480 columns is not reasonable so reducing its size can be helpful especially for reducing memory that is needed for running for database with more image.In comparison with other methods the performance of Normalized LAMSTAR seems to be better and convergence time is pretty much faster than method based on other network such as Back Propagation. Also stability and not being sensitive to initialization are other positive points of using LAMSTAR. Ability to dealing with incomplete and fuzzy input data sets make LAMSTAR neural network an effective candidate for problems such as Iris classification purpose.

REFERENCES

[1] CASIA iris database. Institute of Automation, Chinese Academy of Sciences. http://sinobiometrics.com/casiairis.h

[2] F.Adler, Physiology of the Eye: Clinical Application, fourth ed.

London: The C.V. Mosby Company, 1965.

[3] J.Daugman, Biometric Personal Identification System Based on Iris Analysis, United States Patent, no.5291560, 1994.

[4] J.Daugman, "Statistical Richness of Visual Phase Information: Update on Recognizing Persons by Iris Patterns," Int'l J. Computer Vision, vol. 45, no.1, pp. 25-38, 2001.

[5] H.MiarNaimi, M. Salarian, "A Fast fractal Image Compression Algorithm Using Predefined Values for Contrast Sacaling", Proceedings of the World Congress on Engineering and ComputerScience USA, October-2007.

[6] J.Daugman, "Demodulation by Complex-Valued Wavelets for Stochastic Pattern Recognition", IntJ.Wavelets, Multiresolution and Information Processing, vol.1, no.1, pp.1-17, 2003.

[7] J.Daugman, "How Iris Recognition Works", University of Cambridge, 2001.

[8] Libor Masek. Recognition of Human Iris Patterns for Biometric Identification. School of Computer Science and Soft Engineering, the University of Western Australia, 2003.

[9] Langerudi, Mehran Fasihozaman; Javanmardi, Mahmoud; Mohammadian, Abolfazl (Kouros); Sriraj, PS; "Choice Set Imputation", Transportation Research Record: Journal of the Transportation Research Board,2429,1,79-89,2014,Transportation Research Board of the National Academies,doi:10.3141/2429-09

[10] M Salarian, H Hassanpour, A new fast no search fractal image compression in DCT domain, Machine Vision, 2007. ICMV 2007. International Conference on, 62-66.

[11] Graupe, D.and Kordylewski, H. (1997). A large scale memory (LAMSTAR) neural network for medical diagnosis.In Proceedings of the 19th Annual International Conference of the IEEE Engineering in Medicine and Biology Society. 'Magnificent Milestones and Emerging Opportunities in Medical Engineering',volume 3, pages 1332–5, Piscataway, NJ. IEEE Service Center.

[12] FasihozamanLangerudi, Mehran; HosseinRashidi, Taha;

Mohammadian, Abolfazl; "Investigating the Transferability of Individual Trip Rates: Decision Tree Approach", Transportation Research Board 92nd Annual Meeting, 13-0218, 2013.
[13] http://www.mathworks.com/help/nnet/ug/multilayer-neural-networks.html.
[14] Langerudi, Mehran Fasihozaman; Abolfazl, Mohammadian; Sriraj, PS; "Health and Transportation: Small Scale Area Association", Journal of Transport & Health, 2014, Elsevier,doi:10.1016/j.jth.2014.08.005.
[15] A.Jain, R.Bolle and S. Pankanti, Biometrics: Personal Identification in a Networked Society, Kluwer, 1999.
[16] M Salarian, E Nadernejad and H. M. Naimi, A new modified fast fractal image compression algorithm, Imaging Science Journal, vol. 61, Feb.2013, pp. 219-231, doi: 10.1179/1743131X11Y.0000000027.

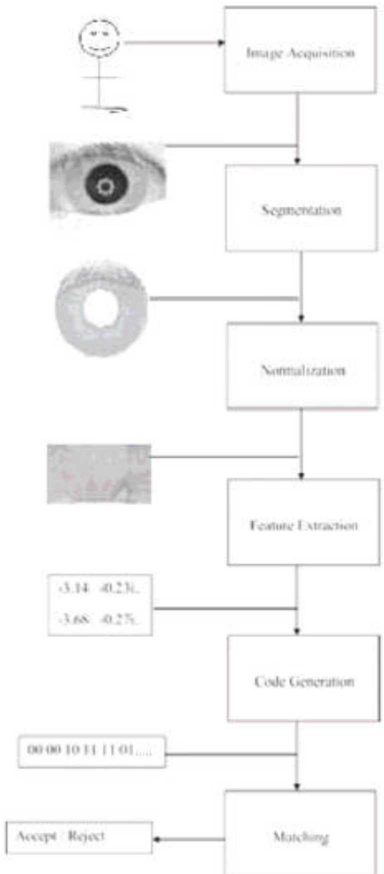

Fig.1. Block diagram of an Iris Recognition

1- Smooth the image with a Gaussian filter (Ref .eq. 1) to reduce noise and unwanted details and textures.

$$G(m,n)=G\ (m,n)*f(m,n)$$

$$\text{Where } G=\frac{1}{2\ c2}\exp\left(\frac{-(m2+n2)}{m2}\right)$$

2- Computer gradient of g(m,n) using any of the gradient operations to get

$$M(n,n) = \sqrt{g^2m(\ m,n) + g\frac{2}{\pi}(m,n)} \text{ and } (m,n) = \tan[\ g\ (\ m,n) / g\ (\ m,n)\ ]$$

3- Threshold M :

$$M\ (\ m,n) = \begin{cases} M(m,n) & M(m,n)>T \\ 0 & \text{otherwise} \end{cases}$$

Where T is so chosen that all edge elements are kept while most of the noise is suppressed .

4- Suppress non-maxima pixels in the edges in M obtained using eq . (3) to thin edge ridges (as the edges might have been broadened in step 1) To do so cheek to see whether each non-zero m (m,n) is greater than its two neighbors ak=long the gradient direction 0 (m,n) . if so keep m (m,n) unchanged otherwise set it to 0

5-Threshold the previous result by two different thresholds T1 and T2 note that compared to t1,t2 has less noise and fewer false edges but larger between edge segments

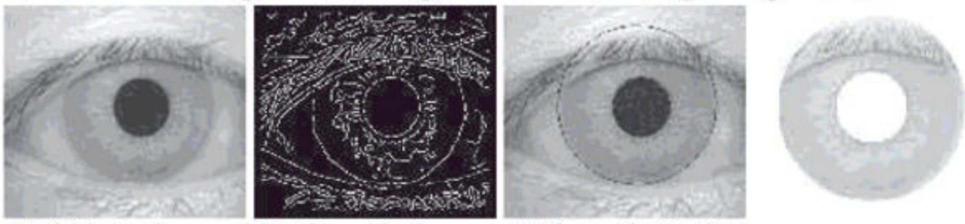

(a) Original eye image (b) After applying Canny edge detector (c) After applying Hough Transform (d) Isolated iris region

2.2 Iris and pupil boundary detection

The Hough transform is a standard computer vision algorithm that can be used to determine the parameters of simple geometric objects, such as lines and circles present in an image. The circular Hough transform is employed to deduce the radius and center coordinates of the pupil and iris regions.

An edge map is generated by calculating the first derivatives of intensity values in an eye image and then thresholding the result. From the edge map, votes are cast in Hough space for the parameters of circles passing through each edge point.These parameters are the center coordinates x_c and y_c and the radius r, which are able to define any circle according to the eq. (4).

$$x_c^2 + y_c^2 - r^2 = 0 \quad (4)$$

A maximum point in the Hough space is corresponding to the radius and center coordinates of the circle best defined by the edge points. Result of Hough transform employed on edge map of the original eye image is shown in Fig. 2(c).

3. Normalization

Once the iris region is successfully segmented from an eye image, the next stage is to transform the iris region so that it has fixed dimensions in order to allow comparisons. The dimensional inconsistencies between eye images are mainly due to the stretching of the iris caused by pupil dilation from varying levels of illumination. Other sources of inconsistency include, varying imaging distance, rotation of the camera, head tilt, and rotation of the eye within the eye socket.

The normalization process will produce iris regions, which have the same constant dimensions, so that two photographs of the same iris under different conditions will have characteristic features at the same spatial location. Another point of note is that the pupil region is not always concentric within the iris region, and is usually slightly nasal. This must be taken into account if trying to normalize the 'doughnut' shaped iris region to have constant radius. Normalization process involves unwrapping the iris and converting it into its polar equivalent as shown in Fig. 3(a). Result of Normalization for the segmented iris for $[0^0, 360^0]$ from the isolated iris region of the original eye image is shown in Fig. 5(a).

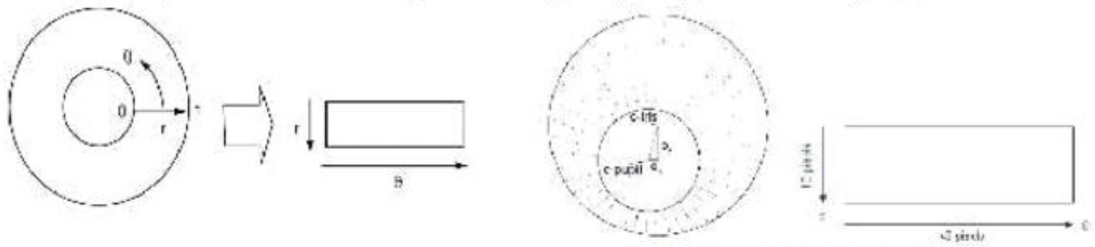

(b) Outline of Normalization Process

The homogenous rubber sheet model devised by Daugman [18] remaps each point within the iris region to a pair of polar coordinates (r,θ) where r is on the interval [0,1] and θ is angle $[0,2\pi]$. The remapping of the iris region from the Cartesian coordinates to the normalized non-concentric polar representation is modelled as in eq. (5).

$$I(x(r,\theta), y(r,\theta)) \rightarrow I(r,\theta)$$

with:

$$x(r,\theta) = (1-r)\, x_p(\theta) + r\, x_i(\theta)$$
$$y(r,\theta) = (1-r)\, y_p(\theta) + r\, y_i(\theta) \quad (5)$$

where $I(x,y)$ is the iris region image, (x,y) are the original Cartesian coordinates, (r, θ) are the corresponding normalized polar coordinates, and x_p, y_p and x_i, y_i are the coordinates of the pupil and iris boundaries along the θ direction. In this model a number of data points are selected along each radial line (defined as the radial resolution).

Consider the center of the pupil as the reference point, and radial vectors pass through the iris region, as shown in Fig. 3(b). The number of radial lines going around the iris region is defined as the angular resolution. Since the pupil can be non-concentric to the iris, a remapping formula is needed to rescale points depending on the angle around the circle and it is given in eq. (6).

$$r' = \sqrt{\alpha\beta} \pm \sqrt{\alpha\beta^2 - \alpha - r_I^2}$$

$$= \cos\left(\pi - \arctan\left(\frac{o_x}{o_y}\right) - \theta\right)$$

Where displacement of the center of the pupil relative to the center of the iris is given by o_x, o_y, and r' is the distance between the edge of the pupil and edge of the iris at an angle, θ around the region, and r_I is the radius of the iris. The remapping formula first gives the radius of the iris region 'doughnut' as a function of the angle θ. A constant number of points are chosen along each radial line, so that a constant number of radial data points are taken, irrespective of how narrow or wide the radius is at a particular angle. The normalized pattern is created by backtracking to find the Cartesian coordinates of data points from the radial and angular position in the normalized pattern. From the 'doughnut' iris region, normalization produces a 2D array, which is shown in Fig. 5(a) with horizontal dimensions of angular resolution and vertical dimensions of radial resolution. In order to prevent non-iris region data from corrupting the normalized representation, data points which occur along the pupil border or the iris border are discarded. As we use Daugman's rubber sheet model, removing rotational inconsistencies is performed at the matching stage during authentication. The normalization process proved to be successful and some results are shown in [18]. However, the normalization process is not able to perfectly reconstruct the same pattern from images with varying amounts of pupil dilation, since deformation of the iris results in small changes of its surface patterns.

Since in most cases the upper and lower parts of the iris area are occluded by eyelid, it is decided to use only the left and right parts of the iris area for iris recognition. Therefore, the whole iris $[0^0, 360^0]$ is not transformed in the proposed system. Experiments are conducted by 32^0 normalization method i.e., normalizing the iris from $[-32^0, 32^0]$ and $[148^0, 212^0]$, ignoring both upper and lower eyelid areas as indicated in Fig. 4. Result of Normalization from $[-32^0, 32^0]$ and $[148^0, 212^0]$ for the segmented iris from the original eye image is shown in Fig. 5(b).

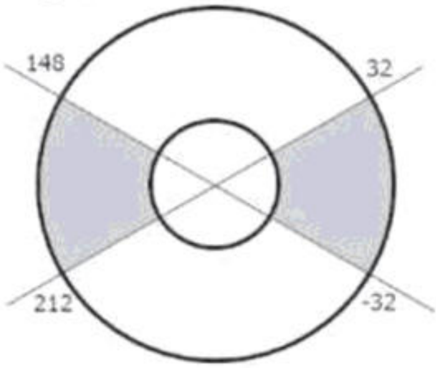

Fig.4. Ignoring Upper and Lower Part of Iris

The size of the rectangular block is reduced accordingly. Left and right side of same iris image of size 86 × 10 is obtained. By applying this approach, detection time of upper and lower eyelids and 64.4% cost of the polar transformation are saved (Ref. Fig. 5). Results have shown that information in these portions of iris is subjective for iris recognition.

(a) Normalized iris for [0^0, 360^0]

(b) Normalized iris from [-32^0, [148^0, 212^0].

. Feature extraction

In order to provide accurate recognition of individuals, the most discriminating information present in an iris pattern must be extracted. Only the significant features of the iris must be encoded so that comparisons between templates can be made. Most iris recognition systems make use of a band pass decomposition of the iris image to create a biometric template. The template that is generated in the feature encoding process is also need a corresponding matching metric, which gives a measure of similarity between two iris templates. This metric should give one range of values when comparing templates generated from the same eye, known as intra-class comparisons, and another range of values when comparing templates created from different irises, known as inter-class comparisons. These two cases should give distinct and separate values, so that a decision can be made with high confidence as to whether two templates are from the same iris, or from two different irises. Feature extraction is implemented by convolving the normalized iris pattern with 1D Log-Gabor wavelets. The 2D normalized pattern is broken up into a number of 1D signal, and then these 1D signals are convolved with 1D Log-Gabor wavelets using FFT and inverse FFT.

Gabor filters are able to provide optimum conjoint representation of a signal in space and spatial frequency. A Gabor filter is constructed by modulating a sine/cosine wave with a Gaussian. This is able to provide the optimum conjoint localization in both space and frequency, since a sine wave is perfectly localized in frequency, but not localized in space. Modulation of the sine with a Gaussian provides localization in space, though with loss of localization in frequency. Decomposition of a signal is accomplished using a quadrature pair of Gabor filters. A disadvantage of the Gabor filter is that the even symmetric filter will have a DC component whenever the bandwidth is larger than one octave [19]. However, zero DC components can be obtained for any bandwidth by using a Gabor filter which is Gaussian on a logarithmic scale this is known as the Log-Gabor wavelet filter. The frequency response of a Log-Gabor wavelet filter is given in eq. (7).

$$G(f)= \exp\left(\frac{-(\log(\frac{f}{f_0}))^2}{2(\log(\frac{\sigma}{f_0}))^2} \right)$$

Where f_0 represents the centre frequency, and σ gives the bandwidth of the filter. Details of the Log-Gabor wavelet filter are examined by Field [19].

Where $\omega_N = e^{\frac{-2\pi i}{N}}$ is an N^{th} root of unity.

The feature extraction process is illustrated in the Fig. 6. Feature extraction is implemented by convolving the normalized iris pattern with 1D Log-Gabor wavelets. The 2D normalized pattern is broken up into a number of 1D signal, and then these 1D signals are convolved with 1D Log-Gabor wavelets using FFT and inverse FFT. The rows of the 2D normalized pattern are taken as the 1D signal; each row corresponds to a circular ring on the iris region.

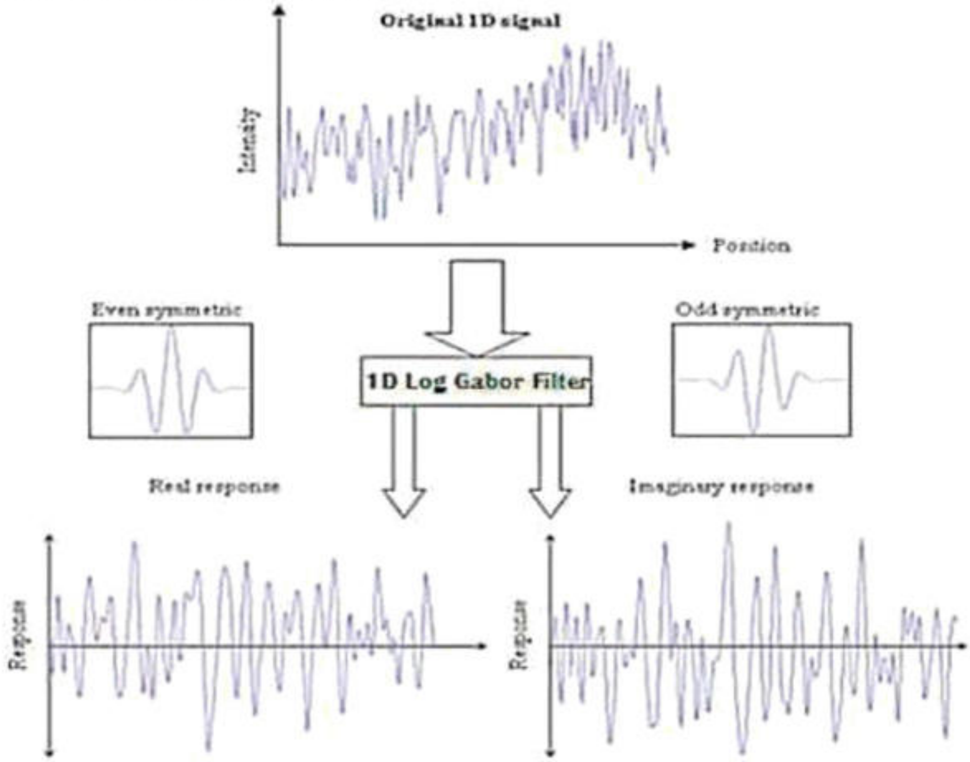

Fig.6.An illustration of the feature extraction process

The angular direction is taken rather than the radial one, which corresponds to columns of the normalized pattern, since maximum independence occurs in the angular direction. The intensity values at known noise areas in the normalized pattern are set to the average intensity of surrounding pixels to prevent influence of noise in the output of the filtering. This process can be explained with the following example. Assume a 6 X 6 matrix from normalized iris, as follows

120	125	150	160	150	120
120	123	156	166	156	120
125	125	155	165	155	120
124	124	154	164	154	120
122	122	152	162	152	120
127	127	157	167	157	120

After convolution with 1D Log-Gabor wavelet filter using FFT and inverse FFT, complex number matrix is produced as features.

-3.14 -i0.23	-1.44 -i2.82	1.75 -i2.69	3.23 +i0.17	1.44 +i2.92	-1.84 +i2.64
-3.68 -i0.27	-1.67 -i3.31	2.06 -i3.14	3.76 +i0.21	1.68 +i3.42	-2.15 +i3.10
-3.33 -i0.23	-1.58 -i3.00	1.86 -i2.92	3.48 +i0.17	1.55 +i3.15	-1.98 +i2.82
-3.32 -i.018	-1.61 -i2.97	1.82 -i2.92	3.46 +i0.14	1.57 +i3.11	-1.93 +i2.82
-3.28 -i0.09	-1.66 -i2.89	1.73 -i2.92	3.14 +i0.07	1.61 +i3.02	-1.82 +i2.82
-3.37 -i0.32	-1.53 -i3.07	1.95 -i2.92	3.53 +i0.25	1.51 +i3.25	-2.09 +i2.82

5. Iris code generation

The feature extracted using 1D Log-Gabor wavelet filter, FFT and IFFT is given as the input to the phase quantization process to produce the template with binary values of 0's and 1's. This result is also known as Iris Code.

Once the iris feature is extracted the output is given to the code generation, here we use the technique called phase quantization for generating the Iris Code. In the Phase Quantization, if both real and imaginary parts are +ve, 11 is assigned. If both real part and imaginary parts are –ve then the 00 is assigned. As well as, if the real part is +ve and imaginary part is –ve, 10 is assigned and if the real part is -ve and imaginary part is +ve , 01 is assigned. Based on the logic shown in Fig.7 iris code is generated as 1's and 0's stream.

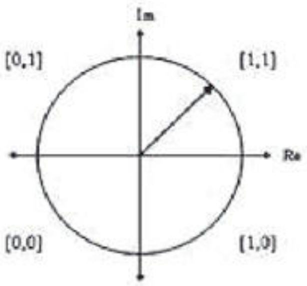

The output of feature extraction is phase quantized to four levels [21], with each filter producing two bits of data for each pixel. The output of phase quantization is chosen to be a grey code, so that when going from one quadrant to another, only 1 bit changes as like following.

00	00	10	11	11	01
00	00	10	11	11	01
00	00	10	11	11	01
00	00	10	11	11	01
00	00	10	11	11	01
00	00	10	11	11	01

This minimizes the number of bits disagreeing, if say two intra-class patterns are slightly misaligned and thus provide more accurate recognition. The encoding process produces a bitwise template containing a number of bits of information, even though the phase information is meaningless at regions where the amplitude is zero. The total number of bits in the template is twice the product of the angular resolution times and the radial resolution times.

6. Iris matching

For matching, the Hamming distance is chosen as a metric for recognition, since bit-wise comparisons are necessary. The Hamming distance algorithm employed in such that only significant bits are used in calculating the Hamming distance between two iris codes. The Hamming distance gives a measure of how many bits are not same between two bit patterns. Using the Hamming distance of two bit patterns, a decision can be made as to whether the two patterns were generated from different irises or from the same one. In comparing the bit patterns X and Y, the Hamming distance, HD, is defined as the sum of disagreeing bits (Ref. eq. 10) i.e., Sum of the exclusive-OR between X and Y over N, the total number of bits in the bit pattern.

N

HD Criterion	Observed False Match Rate
0.220	*0 (thoer: 1 in 5 x 10^{15})*
0.225	*0 (thoer: 1 in 1 x 10^{15})*
0.230	*0 (thoer: 1 in 3 x 10^{14})*
0.235	*0 (thoer: 1 in 9 x 10^{13})*
0.240	*0 (thoer: 1 in 3 x 10^{13})*
0.245	*0 (thoer: 1 in 8 x 10^{12})*
0.250	*0 (thoer: 1 in 2 x 10^{12})*
0.255	*0 (thoer: 1 in 7 x 10^{11})*
0.262	*1in 200 billion*
0.267	*1in 50 billion*
0.272	*1in 13 billion*
0.277	*1in 2.7 billion*
0.282	*1in 284million*
0.287	*1in 96 million*
0.292	*1in 40 million*
0.297	*1in 18 million*
0.302	*1in 8 million*
0.307	*1in 4 million*
0.312	*1in 2 million*
0.317	*1in 1 million*

If two bits patterns are completely independent, such as iris templates generated from different irises, the Hamming distance between the two patterns should equal 0.5. This occurs because independence implies the two bit patterns will be totally random, so there is 0.5 chance of setting any bit to 1, and vice versa. Therefore, half of the bits will agree and half will disagree between the two patterns.If two patterns are derived from the same iris, the Hamming distance between them will be close to 0.0, since they are highly correlated. The False Match Rates, Either Observed in the Distribution of

Fig. 8. Since, Phase Quantization generates two bits of information from one pixel of the normalized region, here two bits are shifted.

The lowest Hamming distance, in this case zero, is then used since this corresponds to the best match between the two templates. The matching process is illustrated in Fig. 9. We suggest the threshold (TH) for HD as 0.10 for CASIA-IrisV3-Interval and 0.25 for UBIRIS (Ref. Fig. 11), so if the HD value is less than TH is nearly matching, if the HD value is 0.0 is exactly matching and if the HD value is more than TH is not matching. Based on this threshold value of HD, Iris Matcher accepts/rejects the personal identification.

7. Experimental result

There are presently 7 public and freely available iris image databases for biometric purposes: Chinese Academy of Sciences (CASIA) [23], Multimedia University (MMU) [24], University of Bath (BATH) [25], Palacký University Olomouc (UPOL) [26], Iris Challenge Evaluation (ICE) [27], West Virginia University (WVU) [28] and University of Beira Interior (UBIRIS) [29]. CASIA database is by far the most widely used for iris biometric purposes. However, its images incorporate few types of noise, almost exclusively related with eyelid and eyelash obstruction, similarly to the images of the MMU and BATH databases. UPOL images are captured with an optometric framework, obtaining noise-free images with extremely similar characteristics. ICE and WVU images contain several blurred and off-angle images, which are noise factors that are out of the scope of this work. Oppositely, UBIRIS database is built with the objective of simulate non cooperative image capturing. This explains the higher heterogeneity of its images and the existence of large noisy regions (iris reflections and obstructions). The aforementioned characteristics led us to choose UBIRIS and CASIA databases for our experiments, analyzing the recognition accuracy both in highly (UBIRIS) and less noisy (CASIA) imaging environments.

We selected 400 images from each database, belonging to 40 subjects. As illustrated by Fig. 10, images of the UBIRIS database contain severe iris obstructions by eyelids and eyelashes in the lower and upper iris regions (regions 1) and specular and lighting reflections predominant in the left and right iris extremes (regions 2). Images of the CASIA database are less noisy and typically contain small iris obstructions due to eyelids and eyelashes in the lower and upper iris regions (regions 1). To eliminate the regions 1 type of noise, we introduced the 32^0 normalisation method. Subsequently this saves detection time of upper and lower eyelids and 64.4% cost of the polar transformation.

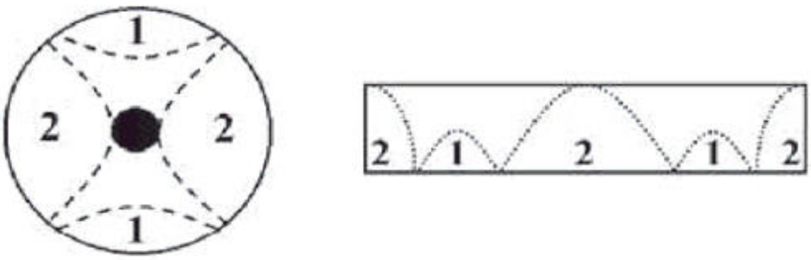

Typical noisy regions in the tested iris images b) Correspondent noisy regions in the segmented and normalized iris images

Fig. 10.Correspondence between the predominant noisy regions of the data set Images

The experiments are completed in two modes: one is verification (one to one matching), the other is identification (one to many matching). In verification mode, we first use the detection error trade-off curves (DET's) to evaluate the performance of our method with Daugman's method. In identification mode, the algorithm is measured by correct recognition rate.

In verification mode, each iris image in the database is compared with the other entire iris. For the public database CASIAIrisV3, we choose 200 classes (eyes) and 1500 images in the subset labelled as CASIA-IrisV3-Interval. The total number of comparisons is (1500 X1499)/2 = 1, 124, 250, where the total number of intra-class comparisons is 7648 and that of inter-class comparisons is 1,116,602. For the database UBIRIS, we choose 200 classes (eyes) and 1000 images. The total number of comparisons is (1000 X999)/2 = 499,500, where the total number of intra-class comparisons is 2000 and that of inter-class comparisons is 497,500. Fig. 11 shows distributions of intra-class and inter-class matching distance in two databases. From the results shown in Fig. 11, we can find that the distance between the intra-class and the inter-class distribution is large, and the portion that overlaps between the intra-class and the inter-class is very small. This proves that the proposed features are highly discriminating.

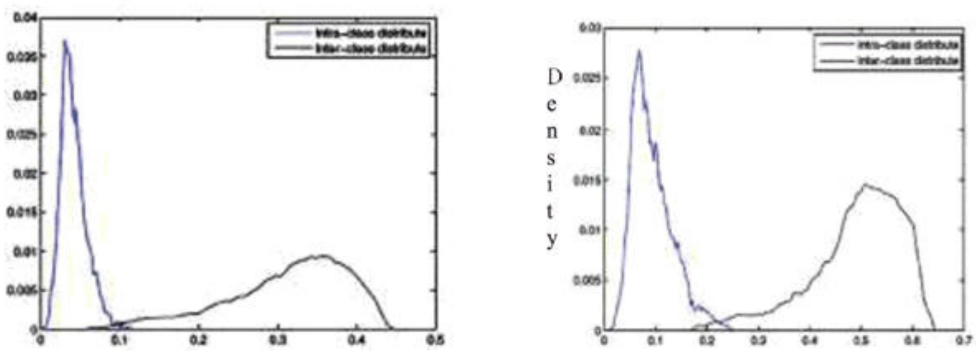

Hamming Distance
CASIA-IrisV3 database

Hamming Distance
b) UBIRIS database

Fig. 11.Distributions of intra-class and inter-class distance

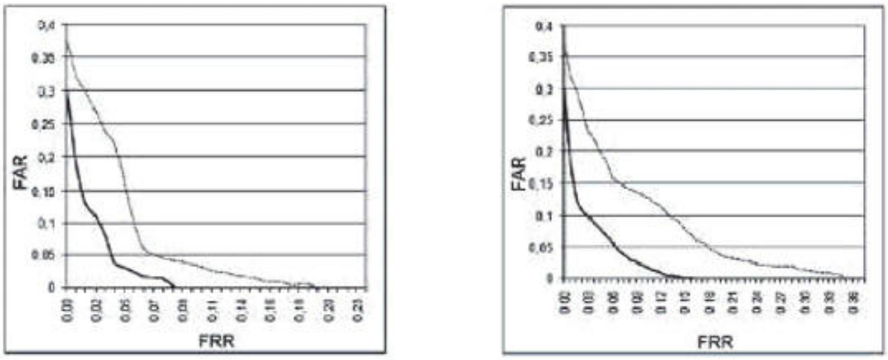

CASIA-IrisV3 database

UBIRIS database

Fig. 12. DET's curve Comparison

Fig. 12 compares the DET's obtained by the Daugman recognition method when using the complete feature set (dashed lines) and our proposed method (continuous lines) for both iris databases. A significant decrement of the error rates is observed, which led us to conclude that our proposal contributes for the adaptability of the recognition system to the typical image noisy regions and increases the recognition robustness to noise.

We also test our method in identification mode. For each iris class, we choose four samples for testing. One hundred percent correct recognition rates are obtained on CASIA-IrisV3 data sets. The feature dimensions used in Daugmans and our method are 2048 and 860, respectively. Therefore, the number of the feature dimensions used in our method is almost one third of Daugman's.

8. Conclusion

Under less constrained lighting environments, it is expected that the captured iris images contain several types of noise. Moreover, the predominant noisy regions are strongly determined by the environment lighting conditions. Due to the huge number of features, traditional feature selection methods are difficult to apply, so we segmented the iris by a simple and fast technique, which is based on Canny edge detector and Hough transform and introduced the 32^0 normalisation method to eliminate Regions 1 type of noise. Consequently, the detection time of upper and lower eyelids and 64.4% cost of the polar transformation are saved. Compared with Daugman's method, a significant decrement of the error rates is observed, which led us to conclude that our proposal contributes for the adaptability of the recognition system to the typical image noisy regions and increases the recognition robustness to noise. As a conclusion remarks, it can be stated that Daugman's method is only suitable for low noise, while the proposed method is suitable for all types of common applications. Particularly well suited for Personal Identification System, since the feature dimensions of the proposed method are almost one third of those used in Daugman's method, ultimately it reduces the storage requirement of the PIS.

Acknowledgements

Portions of the research in this paper used the CASIA iris image database collected by Institute of Automation, Chinese Academy of Sciences and UBIRIS iris database collected by H. Proença and L.A. Alexandre, University of Beira Interior

References

[1] J. Daugman, High confidence visual recognition of personals by a test of statistical independence, IEEE Trans. PAMI; 1993, vol. 15, no. 11, p. 1148–1160.

[2] T. Mansfield, G. Kelly, D. Chandler, and J. Kane, Biometric product testing final report, National Physical Laboratory of UK; March 2001.

[3] L. Ma, Y. Wang, T. Tan, D. Zhang, Personal identification based on iris texture analysis. IEEE Trans Pattern Ana l. Mach. Intel.; 2003, vol. 25, no. 12, p. 1519–1533.

[4] J. Daugman, How iris recognition works, Proceedings of International Conference on Image Processing; 2002.

[5] G. Zhang, M. Salganiciff, Method of measuring the focus of close-up images of eyes, US Patent no.5953440; 1999.

[6] E. Lee, K. Park, and J. Kim, Fake iris detection by using purkinje image, Advances in Biometrics; 2005, vol. 3832, p. 397 – 403.

[7] S. Lee, K. Park, and J. Kim, Robust fake iris detection based on variation of the reflectance ratio between the iris and the sclera, Biometric Consortium Conference, Biometrics Symposium; 2006, p. 1–6.

[8] Z. Wei, X. Qiu, Z. Sun, and T. Tan, Counterfeit iris detection based on texture analysis, ICPR; 2008, p. 1–4.

[9] Z. He, Z. Sun, T. Tan, and Z. Wei, Efficient iris spoof detection via boosted local binary patterns, ICB; 2009, p. 1087– 1097.

[10] J. Daugman, Biometric personal identification system based on iris analysis, Patent no. 5291560; 1994.

[11]R. P. Wildes, J. C. Asmuth, J. K. Hanna, S. C. Hsu, R. J. Kolezynski, J. R. Matey, S. E. McBride, Automated non-invasive iris recognition system and method, Patent no. 5572596; 1996.

[12] W. W. Boles, B. Boashash, A human identification technique using images of the iris and wavelet transform, IEEE Trans Signal Process; 1998, vol. 46, no. 4, p. 1185–1188.

[13] Y. Zhu, T. Tan, Y. Wang, Biometric personal identification based on iris patterns, Proc. Int. Conf. Pattern Recognition; 2000, p. 805–808.

[14] S. Lim, K. Lee, O. Byeon, T. Kim, Efficient iris recognition through improvement of feature vector and classifier, ETRI J; 2001, vol. 23, no. 2, p. 61–70.

[15] C. Tisse, L. Martin, L. Torres, M. Robert, Person identification technique using human iris recognition, Proc. Vis Interface; 2002, p. 294–299.

[16] L. Ma, Y. Wang, T. Tan, Iris recognition based on multichannel Gabor filtering, Proceedings of ACCV'2002, the 5th Asian conference on computer vision;2002, pp. 23–25.

[17] L. Ma, Y. Wang, T. Tan, Iris recognition using circular symmetric filters, Proc. Int. Conf. Pattern Recognition; 2002, p. 414–417.

[19]D. Field, Relations between the statistics of natural images and the response properties of cortical cells, Journal of the Optical Society of America; 1987.

[20] P. Duhamel, and M. Vetterli, Fast Fourier Transforms: A Tutorial Review and a State of the Art, Signal Processing; 1990, vol. 19, p. 259-299.

[21] J. Daugman, New Methods in Iris Recognition, IEEE transactions on systems, man, and cybernetics—part b: cybernetics; 2007, vol. 37, p. 1167-1175.

[22] J. Daugman, Probing the Uniqueness and Randomness of IrisCodes: Results From 200Billion Iris Pair Comparisons, Proceedings of the IEEE; 2006, vol. 94, p. 1927-1935.

[23] CASIA-IrisV3, Inst. of Automation, Chinese Academy of Sciences, http://www.cbsr.ia.ac.cn/IrisDatabase.htm; 2006.

[24] Multimedia University, MMU iris image database, http://pesona.mmu.edu.my/ccteo; 2004.

[25] University of Bath, University of Bath iris image database, http: //www.bath.ac.uk/elec-eng/pages/sipg/; 2004.

[26] M. Dobes and L. Machala, UPOL Iris Image Database, http://phoenix.inf.upol.cz/iris/; 2004.

[27] National Institute of Standards and Technology, Iris challenge evaluation, http://iris.nist.gov/ICE/; 2006.

[28] A. Ross, S. Crihalmeanu, L. Hornak, and S. Schuckers, A centralizedweb-enabled multimodal biometric database, In Proceedings of the 2004Biometric Consortium Conference (BCC), U.S.A; 2004.

[29] H. Proença and L.A. Alexandre, UBIRIS: A Noisy Iris Image Database, http://iris.di.ubi.pt; 2005.

SUPERVISOR CERTIFICATION

I certify that the preparation of this project entitled

A personal Identification System Using Iris Recognition

prepared by

1-naba jasim mohammed

2_hadeer mohaned adnan

3-Surror naseer mohammed ali

was made under my supervision in the Department of Computer Science/College of Science/University of Diyala and it is part of the requirements for obtaining a Bachelor's degree in Computer Science

Signature:
Name :
Date:

((الخـــاتمــــــــــة))

احدث التقدم التكنلوجي ثورة في مجال الحاسب
والمعلومات وساهم في تقدم التقني . وللتعرف على
مدى مواكبة هذا العنصر للتطورات التكنلوجية
الحديثة من حيث مصادر المعلومات الالكترونية وقد
حاولنا في مشروعنا في تقديم نموذج مبسط للتعرف
على الاشخاص من خلال قزحية العين من نواحي
مفيدة جدا تسهيل الوقت والجهد لمستخدم البرنامج
.واشكر كل من ساعدني ووجهي في اعداد هذا المشروع
الذي اتمنى ان ينفعنا الله به والمسلمين
وفي النهاية نتمنى ان ينال المشروع الرضى والقبول
ونسأل الله العلي والقدير ان ينفعنا بما علمنا وان
يردينا علما .

((إقرار المشرف))

اشهد بأن اعداد هذا المشروع الموسوم

نظام التعرف على الاشخاص من خلال قزحية العيون

والمعد من قبل الطلاب

١- نبأ جاسم محمد
٢- هدير مهند عدنان
٣- سرور نصير محمد علي

قد تم تحت أشرافي في قسم علوم الحاسوب / كلية العلوم/ جامعة ديالى وهي جزء من متطلبات نيـــــل شهادة البكالوريوس في اختصاص علوم الحاسوب

التوقيع:
الاسم:
المرتبة العلمية :

: التاريخ